

Realizing Quantum Controlled Phase Flip through Cavity-QED

Yun-Feng Xiao,^{*} Xiu-Min Lin, Jie Gao, Yong Yang, Zheng-Fu Han,[†] and Guang-Can Guo[‡]

*Key Laboratory of Quantum Information,
University of Science and Technology of China (CAS),
Hefei 230026, People's Republic of China.*

Abstract

We propose a scheme to realize quantum controlled phase flip (CPF) between two rare earth ions embedded in respective microsphere cavity via interacting with a single-photon pulse in sequence. The numerical simulations illuminate that the CPF gate between ions is robust and scalable with extremely high fidelity and low error rate. Our scheme is more applicable than other schemes presented before based on current laboratory cavity-QED technology, and it is possible to be used as an applied unit gate in future quantum computation and quantum communication.

PACS numbers: 03.67.Lx, 32.80.Qk, 42.50.-p

^{*}Electronic address: yfxiao@mail.ustc.edu.cn

[†]Electronic address: zfhan@ustc.edu.cn

[‡]Electronic address: gcguo@ustc.edu.cn

I. INTRODUCTION

Quantum computation based on cavity quantum electrodynamics (QED) [1, 2] attracts persistent interest in experimental realization [3, 4, 5, 6, 7]. In theory, cavity-QED with long-lived states and high- Q cavities thus provides a promising tool for creating entanglement and superposition, and also for implementation of quantum computing algorithms. In a number of different schemes, quantum information usually can be represented by states of photons [3, 4] or atomic/ionic states [5, 6, 7]. In a classical quantum computation scheme based on cavity-QED of Ref. [3], qubits are represented by the polarized states of photons, and high-finesse optical microcavities with atoms are used to provide nonlinear interactions between photons. However, the storage of single-photon information and feeding of single photons into/out of cavities are still experimental challenges for large-scale quantum computation. In the other case, qubits are represented by atomic states, which are ideal for the storage of quantum information, and photons transmit information among atoms, which are the best long-distance carriers of quantum information. An important precondition for the case is so-called regime of strong coupling in cavity-QED. Experimentally, the condition has been realized [1, 2] or is theoretically feasible in different optical cavities, such as micropost microcavity [8], Fabry-Perot bulk optical cavity [9], photonic crystal [10] and microsphere cavity [11], etc. Among them, whispering gallery modes of silica-microsphere get especial attentions because of their ultrahigh factor Q and small mode volume.

Very recently, L.-M. Duan and H. J. Kimble have proposed a new interesting scheme to carry out quantum controlled phase flip (CPF) [12], where qubits are encoded as coherent superposition of polarized states of single-photon pulses. They assumed $T \gg 1/\kappa$, which means longer storage time of single photons is needed, and thus it brings on a challenge for maintaining photons coherent, and here κ is the decay rate of the cavity mode field itself, and T is the single-photon pulse duration. The experimental scheme presented here tries to overcome these difficulties by using atomic rare earth ions embedded in microsphere cavities. Qubits are represented by hyperfine ground states of ions, which provides less storage time of single-photon pulses and better scalability.

II. IMPLEMENTATION OF CPF GATE

The basic model here is first built on single three-level atoms trapped in Fabry-Perot cavities, and single three-level ions embedded in microsphere cavities will be discussed in the section IV later. As illustrated in Fig. 1a, atomic states $|0\rangle$ and $|1\rangle$ are two stable ground states, and state $|e\rangle$ is a low excited state. A single-photon pulse is reflected by the two cavity-atom subsystems in sequence, and the CPF gate for the two atoms is realized by a series of these simple reflections and some local unitary operations. The single-photon pulse is initially prepared in an equal coherent superposition of two orthogonal polarization components and can be expressed as $|\phi\rangle_p = \frac{1}{\sqrt{2}}(|H\rangle + |V\rangle)$. Qubits are represented by arbitrary coherent superposition of the two atomic ground states, and the initial state is prepared as $|\varphi\rangle_{12} = (\beta_{10}|0\rangle_1 + \beta_{11}|1\rangle_1) \otimes (\beta_{20}|0\rangle_2 + \beta_{21}|1\rangle_2)$, where β_{ij} is arbitrary superposition coefficients, i denotes the *atom1* or *atom2*, j denotes the state $|0\rangle$ or $|1\rangle$, with relations: $|\beta_{i0}|^2 + |\beta_{i1}|^2 = 1$. The atomic transition $|1\rangle \rightarrow |e\rangle$ is resonant with a cavity mode of interest, which has H polarization and is resonantly driven by the H polarization component of the input single-photon pulse. The CPF gate between the atom and the photon can be described by the unitary operator [12]

$$U_{a,p}^{CPF} = e^{i\pi|0\rangle_i\langle 0|\otimes|H\rangle_p\langle H|}. \quad (1)$$

From Eq. (1), $|0\rangle$ component obtains a phase of $e^{i\pi}$ while $|1\rangle$ component keeps unchanged during the interaction with H polarization component of the input single-photon pulse. It is very insensitive to the variation of the coupling rate g even if g is not much higher than κ [12]. The CPF gate between *atom1* and *atom2*, which is generated by combination of several gates $U_{a,p}^{CPF}$ and single-bit rotation operations can be described by the unitary operator

$$U_{12}^{CPF} = e^{i\pi|0\rangle_1\langle 0|\otimes|0\rangle_2\langle 0|}. \quad (2)$$

It is the most important unitary operator in our protocol which has the following operator identity

$$U_{12}^{CPF} |\varphi\rangle_{12} |\phi\rangle_p = U_{1p}^{CPF} R_p U_{2p}^{CPF} R_p U_{1p}^{CPF} |\varphi\rangle_{12} |\phi\rangle_p. \quad (3)$$

where R_p is a single-bit operating on the single-photon pulse, and the transforming relations are $R_p|H\rangle = \frac{\sqrt{2}}{2}(-|H\rangle + |V\rangle)$ and $R_p|V\rangle = \frac{\sqrt{2}}{2}(|H\rangle + |V\rangle)$. So the steps to realize the CPF gate between *atom1* and *atom2* are as follows, and the overall processes are shown in

Fig. 1b. (i). *cavity1* with *atom1* reflects the input single-photon pulse firstly. (ii). Make a rotation R_p on the polarization direction of the single-photon pulse via a half-wave plate *HWP1*. (iii). *cavity2* with *atom2* reflects the single-photon pulse subsequently. (iv). Make a rotation R_p on the polarization direction of the single-photon pulse via the other half-wave plate *HWP2*. (v). *cavity1* with *atom1* reflects the single-photon pulse again, and then the single-photon pulse leaves the setup. At last, the state of the two atoms is expressed by

$$|\varphi\rangle'_{12} = -\beta_{10}\beta_{20} |0\rangle_1 |0\rangle_2 + \beta_{10}\beta_{21} |0\rangle_1 |1\rangle_2 + \beta_{11}\beta_{20} |1\rangle_1 |0\rangle_2 + \beta_{11}\beta_{21} |1\rangle_1 |1\rangle_2, \quad (4)$$

and meanwhile the single-photon pulse comes back to its initial state $|\phi\rangle_p$.

III. THEORETICAL MODEL AND ANALYSIS

For the sake of clarity and concision, we discuss $U_{a,p}^{CPF}$ for a single-photon pulse and a cavity-atom subsystem, and CPF gate between atoms is generated by simple orderly combination of $U_{a,p}^{CPF}$ and some local unitary operations. The total Hamiltonian (single atom + single cavity mode + free space) has the following form in the rotating frame [13] (in the units of $\hbar = 1$, and input single-photon pulse is H polarized)

$$\begin{aligned} \mathbf{H} = & -i\frac{\gamma}{2} |e\rangle \langle e| + g \left(a_H |e\rangle \langle 1| + |1\rangle \langle e| a_H^\dagger \right) + \int_{-\omega_b}^{\omega_b} d\omega [\omega b^\dagger(\omega) b(\omega)] \\ & + i\sqrt{\kappa/2\pi} \int_{-\omega_b}^{\omega_b} d\omega \left[b(\omega) a_H^\dagger - a_H b^\dagger(\omega) \right], \end{aligned} \quad (5)$$

where γ is atomic spontaneous rate in state $|e\rangle$; a_H and $b(\omega)$ are respectively annihilation operators for H polarized photons in the cavity mode and in free-space modes with the commutation relation: $[b(\omega), b^\dagger(\omega')] = \delta(\omega - \omega')$. Here ω_b is a frequency range around the frequency of the cavity mode. In order to obtain the state of the system at arbitrary time, two cases are considered:

1. The atom is in $|0\rangle$ state at the beginning, then the state at arbitrary time is described by

$$|\Phi(t)\rangle = |0\rangle_{atom} |vac\rangle_{cavity} \int_{-\omega_b}^{\omega_b} d\omega c_\omega(t) b^\dagger(\omega) |vac\rangle_{freespace} + \lambda(t) |0\rangle_{atom} |H\rangle_{cavity} |vac\rangle_{freespace}. \quad (6)$$

According to Schrödinger equation $i\partial_t |\Phi(t)\rangle = \mathbf{H} |\Phi(t)\rangle$, we have

$$\begin{cases} dc_\omega(t)/dt = -i\omega c_\omega(t) - \sqrt{\kappa/2\pi} \lambda(t), \\ d\lambda(t)/dt = \int_{-\omega_b}^{\omega_b} d\omega \sqrt{\kappa/2\pi} c_\omega(t). \end{cases} \quad (7)$$

Then we discretize the continuum field $b(\omega)$ for the numerical simulation with the single-photon pulse state replaced by $|\phi'\rangle_p = \sum_{k=1}^N c_k(t) b_k^\dagger |vac\rangle$, and finally we get the following set of equations for the coefficients

$$\begin{cases} dc_k(t)/dt = -i\omega_k c_k(t) - \sqrt{\kappa\Delta\omega/2\pi}\lambda(t), \\ d\lambda(t)/dt = \sqrt{\kappa\Delta\omega/2\pi} \sum_{k=1}^N c_k(t), \end{cases} \quad (8)$$

where $N = 2\omega_b/\Delta\omega$, $\omega_k = [k - (N + 1)/2]\Delta\omega$, and at time $t = 0$, we have $\lambda(0) = 0$, $c_k(0) = \sqrt{\Delta\omega}c_\omega(0)$. Shape of the input single-photon pulse is described by a Gauss function $f(t) = \alpha \exp[-24(t - T/2)^2/T^2]$ ($t \in [0, T]$).

2. The atom is in state $|1\rangle$ initially. Similar treatments can be done, and thus we have

$$|\Phi'(t)\rangle = |1\rangle |vac\rangle \int_{-\omega_b}^{\omega_b} d\omega c'_\omega(t) b^\dagger(\omega) |vac\rangle + \lambda'(t) |1\rangle |H\rangle |vac\rangle + \mu(t) |e\rangle |vac\rangle |vac\rangle, \quad (9)$$

and

$$\begin{cases} dc'_k(t)/dt = -i\omega_k c'_k(t) - \sqrt{\kappa\Delta\omega/2\pi}\lambda'(t), \\ d\lambda'(t)/dt = \sqrt{\kappa\Delta\omega/2\pi} \sum_{k=1}^N c'_k(t) - ig\mu(t), \\ d\mu(t)/dt = -ig\lambda'(t) - (\gamma/2)\mu(t), \end{cases} \quad (10)$$

where $\lambda'(0) = \mu(0) = 0$, $c'_k(0) = c_k(0)$.

In fact, the initial atomic state in our scheme is an arbitrary coherent superposition of the two ground states, $|\varphi\rangle_a = (\beta_0 |0\rangle + \beta_1 |1\rangle)$ and the input single-photon pulse is $|\phi\rangle_p = \frac{1}{\sqrt{2}}(|H\rangle + |V\rangle)$, so final state of total system can be expressed as

$$|\Xi(t)\rangle_{total} = \frac{1}{\sqrt{2}} (\beta_0 |\Phi(t)\rangle + \beta_1 |\Phi'(t)\rangle + \beta_0 |0\rangle |vac\rangle |V\rangle + \beta_1 |1\rangle |vac\rangle |V\rangle). \quad (11)$$

Gate fidelity between the atom and the photon is

$$F = \langle \Xi_{a,p}^{Ideal}(T) | \rho_{a,p}(T) | \Xi_{a,p}^{Ideal}(T) \rangle, \quad (12)$$

where $\rho_{a,p}(T) = Tr_{cav}(|\Xi(t)\rangle \langle \Xi(t)|)$ is the reduced density operator of the atom and photon, and $|\Xi_{a,p}^{Ideal}(T)\rangle$ is the final state of atom and photon by ideal $U_{a,p}^{CPF}$ gate, taking the following form

$$\begin{aligned} |\Xi_{a,p}^{Ideal}(T)\rangle &= \frac{1}{\sqrt{2}} \left(-\beta_0 |0\rangle \sum_{k=1}^N e^{-i\omega_k T} c_k(0) b_k^\dagger |vac\rangle + \beta_1 |1\rangle \sum_{k=1}^N e^{-i\omega_k T} c_k(0) b_k^\dagger |vac\rangle \right) \\ &+ \frac{1}{\sqrt{2}} (\beta_0 |0\rangle |V\rangle + \beta_1 |1\rangle |V\rangle). \end{aligned} \quad (13)$$

It corresponds with $\lambda(T) = \lambda'(T) = \mu(T) = 0$, and the factor $e^{-i\omega_k T}$ describes the phase change due to the propagation in vacuum during time T . The fidelity can be written finally

$$\begin{aligned} F &= \frac{1}{2} |\xi_1 x + \xi_2 (1 - x) + 1|^2 \\ &= \frac{1}{4} (s_2 x^2 + s_1 x + s_0), \end{aligned} \quad (14)$$

where $\xi_1 = -\sum_{k=1}^N [e^{-i\omega_k T} c_k(0)]^* c_k(T)$, $\xi_2 = \sum_{k=1}^N [e^{-i\omega_k T} c'_k(0)]^* c'_k(T)$, $x = |\beta_0|^2 = 1 - |\beta_1|^2$, $s_2 = |\xi_1 - \xi_2|^2$, $s_1 = 2 \operatorname{Re}[(\xi_2^* + 1)(\xi_1 - \xi_2)]$, $s_0 = |\xi_2 + 1|^2$. The minimum of the fidelity for $U_{a,p}^{CPF}$ can be expressed as

$$F_{\min} = \begin{cases} \frac{1}{4} s_0, & (-s_1/2s_2 < 0), \\ \frac{1}{4} (s_0 - s_1^2/4s_2), & (0 \leq -s_1/2s_2 \leq 1), \\ \frac{1}{4} (s_0 + s_1 + s_2), & (-s_1/2s_2 > 1). \end{cases} \quad (15)$$

IV. SIMULATION AND DISCUSSION

In order to take numerical simulation for the theoretical results of the previous section, it is necessary to consider a practicable system and take some practical parameter estimations. First of all, we consider silica-microsphere cavities instead of Fabry-Perot cavities for better strong coupling conditions and physical scalability. In the silica-microsphere cavity, whispering-gallery modes (WGMs) are supported. In a ray-optics picture, WGMs correspond to light traveling around the equator of a microsphere, and characterized by mode numbers q, l, m and their polarizations (TE or TM), where q is the radial and l, m are angular mode numbers respectively. What we are most interested in is the so-called fundamental WGM ($q = 1, l = m$) which corresponds to the highest quality factor Q and the smallest volume V_m . Quality factor Q of WGM can reach extremely high, up to 10^{10} in experiments [14], and thus strong coupling conditions are more easily obtained than that by F-P cavity [11]. In the recent work, one group has just mentioned a quantum computation protocol through microsphere-cavity-assisted interaction [15]. In order to achieve good coupling between photons and WGMs, being different from F-P cavity (direct coupling is obtainable through one mirror of the cavity), near field evanescent wave couplers are required to provide efficient coupling without disturbing the high- Q character of the microsphere cavity, and fiber tapers [16] or stripline pedestal anti-resonant reflecting optical waveguides (SPARROW) [17] are usually used for critical coupling [16]. Fig. 2 shows the coupling between two fiber tapers

and a microsphere, i.e. the realization of gate $U_{i,p}^{CPF}$ between an ion and a photon. For a single TE type WGM, the H polarization component of the input pulse can couple into (out of) microsphere cavity via $Taper1$ ($Taper2$), while the V polarization component will pass the coupling region and cannot couple into the microsphere cavity, and in essence, it is equivalent to the reflection by the mirror M . Thus the physical setup is simpler than that of F-P cavity because it has no $C1$, $C2$ and PBS and just need to control the working-state of switches $K1$ and $K2$ with low time precision. Combining the advantages of fiber taper and microsphere cavity, the system not only achieves best coupling efficiency (the efficiency is up to 99.7% when critical coupling is achieved) [16] but also supplies good cascability. Secondly, we replace the neutral atoms by atomic trivalent rare earth ions RE^{3+} (such as Pr^{3+} or Eu^{3+} , here we adopt Eu^{3+}) for longer coherence time and lower spontaneous emission rate. Quantum computation using rare-earth ions have also been proposed by several groups [20]. Quantum information can be stored in the ground state structure for long periods of time (up to 82 ms [19]) and it is insensitive to the electric dipole-dipole interaction. In our scheme, the states $|0\rangle$ and $|1\rangle$ are respectively ${}^7F_0(\pm 5/2)$ and ${}^7F_0(\pm 3/2)$, and $|e\rangle$ is ${}^5D_0(\pm 5/2)$ [18].

We assume a single ion Eu^{3+} lies in the inner surface of the microsphere, which is also the primary distributed position of the fundamental WGM ($q = 1, l = m$). The radii of each microsphere here is about $10 \mu\text{m}$, and mode volume V_m is about $300 \mu\text{m}^3$ at $\lambda_0 = 579.879 \text{ nm}$; the Q factor can be up to 5×10^7 [11]. The maximum coherent coupling rate of an individual ion to the resonant WGM [2] is given by $g_0 = \left(\frac{\mu^2 \omega_c}{2\hbar \epsilon_0 V_m}\right)^{1/2} \approx 1.0 \text{ GHz}$; here we let $\mu \sim er_{ion}/2 \sim 7.5 \times 10^{-19} \text{ C} \cdot \text{nm}$. Decay rate of the mode reaches $\kappa = \omega_0/2Q \sim 32 \text{ MHz}$, and we assume single-photon pulse duration T is about $3.0 \mu\text{s}$ for $\kappa T \gg 1$. Last key parameter about strong coupling conditions is ionic decay rate to modes other than the cavity mode of interest. It is reasonable to assume $\gamma = 1 \text{ kHz}$ here because lifetime of spontaneous emission in the excited state of rare earth can reach several ms [18, 20, 21]. Sum up all the above, $g \gg \kappa \gg \gamma$ can be satisfied in our scheme; i.e., strong coupling between single ion and microsphere cavity mode can be easily realized.

Based on above parameter estimations, we prove that we have realized the CPF gate via numerical simulations. In Fig. 3a, we show ionic phase variation under gate $U_{i,p}^{CPF}$ for different ω_k , $\Delta\theta_{\omega_k}^{(0)} = \theta_{\omega_k}^{(0)}(\text{cavity}) - \theta_{\omega_k}^{(0)}(\text{vac})$ and $\Delta\theta_{\omega_k}^{(1)} = \theta_{\omega_k}^{(1)}(\text{cavity}) - \theta_{\omega_k}^{(1)}(\text{vac})$, where $\theta_{\omega_k}^{(0)}(\text{cavity})$ and $\theta_{\omega_k}^{(1)}(\text{cavity})$ denote final ionic phase after H polarization component of the

photon is reflected by cavity-ion subsystem when the ionic state is $|0\rangle$ or $|1\rangle$, and $\theta_{\omega_k}^{(0)}(vac)$ or $\theta_{\omega_k}^{(1)}(vac)$ are final ionic phases in the absence of cavity-ion subsystem during time T (it means photon's free propagation in vacuum). Thus we have $\theta_{\omega_k}^{(0)}(cavity) = \arg[c_k(T)]$, $\theta_{\omega_k}^{(0)}(vac) = \arg[e^{-i\omega_k T} c_k(0)]$, $\theta_{\omega_k}^{(1)}(cavity) = \arg[c'_k(T)]$, $\theta_{\omega_k}^{(1)}(vac) = \arg[e^{-i\omega_k T} c'_k(0)]$. From the two curves, it is obvious that $\Delta\theta_{\omega_k}^{(0)}$ is very close to π , and $\Delta\theta_{\omega_k}^{(1)}$ nearly equals 0 in the frequency range of single-photon pulse.

We also obtain the fidelity of the CPF gate for a single ion and a single photon. Fig. 3b shows the gate fidelity associated with different pulse duration T . F_{\min} can reach extremely high even when $\kappa T \sim 50$. In our estimations, F_{\min} is up to 0.99998 for $T = 3.0 \mu\text{s}$. The other important parameter of quantum logic gates in quantum computation is error rate. The dominant noise in our scheme is photon loss during gate operations, which is especially aroused from ionic spontaneous emission, and leads to uncontrolled free evolution of ionic states; per contra, ions evolve governed by Hamiltonian \mathbf{H} when the single photon is in the cavity. Taking a rough estimation for this case, probability of spontaneous emission loss (η) is about $\frac{1}{2(1+2g^2/\kappa\gamma)} \approx 10^{-8}$ for per gate $U_{i,p}^{CPF}$ even when $|\varphi\rangle_{ion} = |1\rangle$ [13]. So our scheme has the ability to accomplish quantum fault-tolerance codes (error threshold is about 10^{-5}) [22] if we neglect all classical photon loss (for instance, coupling inefficiency between fiber tapers and microspheres).

Now we discuss some technical details of our scheme. Rare earth ions are characterized by partially full $4f$ orbitals and their spectroscopy is dominated by $4f^n \rightarrow 4f^n$ transitions. The electrons involved in these transitions are inside filled $5s$ and $5p$ orbitals, which screen them from perturbations caused by the lattice [18, 23]. Once a single ion has been embedded in a silica-microsphere, it has nearly determinate crystal field environment, and the fluctuation of its crystal field is so small that linewidths of around 100 Hz for a transition in the visible have been reported [21]. These linewidths are right so-called homogeneous broadening $\Delta\omega_{hb}$. On the other hand, for different ions, they have different crystal field environments and hence different optical transition frequencies. This kind of behavior brings large inhomogeneous broadening $\Delta\omega_{ib}$, up to several GHz [24]. Large inhomogeneous broadening is a significant challenge for our scheme, since single photons should be kept resonant with ionic transitions, but obviously, it is not a natural corollary of the aforementioned protocol. In order to get over the effect derived from this inhomogeneous broadening, we improve our protocol to be more potential. Simply, we could only add two acousto-optical (AO) shifters in fig. 2. One

(AO shifter 1) is in front of the couplers, and the other (AO shifter 2) is mounted rearward. In other words, the single-photon pulse will be modulated in the frequency domain by AO shifters before and after reflection by the cavity. For instance, the central frequency of the transition ($|1\rangle \rightarrow |e\rangle$) is assumed $(\omega_0 + \delta\omega_i)$ for the i th ion. The central frequency of the incident single-photon pulse is ω_0 , and the frequency increases (decreases) $\delta\omega_i$ after it passes through AO shifter 1 (2). In actual quantum computers, we can fabricate a number of microspheres in which single ions are imbedded. Then we analyse their frequency spectrums one by one, and range the ions by their central frequencies by ascending order. Every cavity-ion subsystem includes two additional AO shifters, and thus the single-photon pulse with central frequency ω_0 can sufficiently interact with every ion embedded in the respective microsphere. Furthermore, WGMs in microsphere have been tuned successfully by several methods [25], and thus cavity modes are always able to keep resonant with ionic transitions. On second thoughts, however, we may even design an elegant scheme to use the inhomogeneous broadening as a constructive factor of quantum logic gates, instead of fighting against its destructive characteristic. For instance, we can approximatively consider that each ion has a different discrete linear spectrum described by $(\omega_0 + \delta\omega_i)$ because homogeneous broadening $\Delta\omega_{hb}$ is much narrower than inhomogeneous broadening. Therefore, even single ions to be addressed individually in the case of not knowing the position of every ion. It may be used for addressing, or writing and reading data in future quantum computers.

V. SUMMARY

In conclusion, we have described a scheme to realize quantum computation in current laboratorial technique. Compared with other schemes, our scheme has the following significant advantages: (a) CPF gate between ions has very high fidelity and low error rate. Routinely, in the worst case, $F \gtrsim 0.9999$ and $\eta \lesssim 10^{-8}$ for $U_{i,p}^{CPF}$ are obtainable. (b) Simpler setup but good strong coupling conditions, and we need no measurement [26] and shorter time delay. Our delay time in total process is only T while the time is at least $2T$ in Ref. [12]. (c) Our scheme is scalable because operation times $n_{op} = \tau_{coh}/(2T)$ can be expected about ten thousands, and most remarkably, microsphere cavities themselves tend to be scalable through fiber tapers or SPARROWS. It is stirring that every cavity-ion subsystem possibly represents a node in future quantum information and quantum computation

while single-photon pulse mediates their interaction through fiber taper or SPARROW technique. Quantum computation based on our scheme is more applicable in lab with current experimental technique for we can operate single ions into microsphere cavities more controllably and accurately.

Acknowledgments

We thank Prof. Z.-W. Zhou, for his helpful advice. We also like to thank J.-L. Cheng for his help on numerical simulation. We especially acknowledge fruitful discussions with M.-Y. Ye. This work was funded by National Fundamental Research Program of China (2001CB309300), the Innovation Funds of Chinese Academy of Sciences.

-
- [1] Y. Yamamoto and Richard E. Slusher, *Physics Today* **46**, 66 (1993).
 - [2] H.J. Kimble, *Cavity Quantum Electrodynamics*, edited by Paul R. Berman (Academic Press, Inc., 1994), pp. 203-266.
 - [3] Q.A. Turchette, C.J. Hood, W. Lange, H. Mabuchi, and H.J. Kimble, *Phys. Rev. Lett.* **75**, 4710 (1995).
 - [4] I.L. Chuang and Y. Yamamoto, *Phys. Rev. A* **52**, 3489 (1995).
 - [5] T. Pellizzari, S.A. Gardiner, J.I. Cirac, and P. Zoller, *Phys. Rev. Lett.* **75**, 3788 (1995).
 - [6] J.I. Cirac, P. Zoller, H.J. Kimble, and H. Mabuchi, *Phys. Rev. Lett.*, **78**, 3221 (1997).
 - [7] J. Pachos and H. Walther, *Phys. Rev. Lett.* **89**, 187903 (2002).
 - [8] D. Fattal *et al.*, *Phys. Rev. Lett.* **92**, 037903 (2004).
 - [9] J. McKeever *et al.*, *Phys. Rev. Lett.* **90**, 133602 (2003); J. McKeever *et al.*, *Nature* **425**, 268 (2003).
 - [10] O. Painter *et al.* *Science* **284**, 1819 (1999).
 - [11] K.J. Vahala, *Nature* **424**, 839 (2003); J.R. Buck and H.J. Kimble, *Phys. Rev. A* **67**, 033806 (2003).
 - [12] L.-M. Duan and H.J. Kimble, *Phys. Rev. Lett.* **92**, 127902 (2004).
 - [13] L.-M. Duan, A. Kuzmich, and H.J. Kimble, *Phys. Rev. A* **67**, 032305 (2003).

- [14] M.L. Gorodetsky *et al.*, *Opt. Lett.* **21**, 453 (1996).
- [15] T.A. Brun and H.L. Wang, *Phys. Rev. A* **61**, 032307 (2000); W. Yao, R.-B. Liu, and L.J. Sham, *Phys. Rev. Lett.*, **92**, 217402 (2004).
- [16] M. Cai, O. Painter, and K.J. Vahala, *Phys. Rev. Lett.* **85**, 74 (2000); S.M. Spillane, T.J. Kippenberg, O.J. Painter, and K.J. Vahala, *Phys. Rev. Lett.* **91**, 043902 (2003); M. Cai, thesis for **PH. D**, CIT, 2001.
- [17] J.P. Laine *et al.*, *IEEE Phot. Tech. Lett.* **12**, 1004 (2000).
- [18] J.J. Longdell, thesis for **PH. D**, The Australian National University, 2003.
- [19] E. Fraval, M.J. Sellars, and J.J. Longdell, quant-ph/0306169.
- [20] K. Ichimura, *Opt. Commun.* **196**, 119 (2001); J.J. Longdell and M.J. Sellars, quant-ph/0310105; J. Wesenberg *et al.*, quant-ph/031036; J.J. Longdell *et al.*, quant-ph/0404083.
- [21] R.W. Equall, Y. Sun, R.L. Cone, and R.M. Macfarlane, *Phys. Rev. Lett.* **72**, 2179 (1994).
- [22] <http://www.theory.caltech.edu/people/preskill/ph229>.
- [23] <http://www.physics.montana.edu>.
- [24] G.J. Pryde, M.J. Sellars, and N.B. Manson, *Phys. Rev. Lett.* **84**, 1152 (2000).
- [25] V.S. Ilchenko *et al.*, *Opt. Commun.* **145**, 86 (1998); M.L. Gorodetsky and I.S. Grudinin, cond-mat/0304049.
- [26] Y.-F. Xiao *et al.*, submitted to *Phys. Lett. A*.

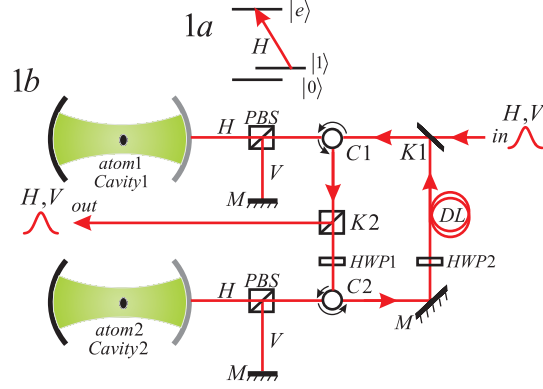


FIG. 1: (a) The energy level diagram of atoms. $|1\rangle \rightarrow |e\rangle$ is resonant with the bare cavity mode. (b) Schematic setup to realize CPF gate between *atom1* and *atom2*. Both atoms lie in the two microcavities *cavity1* and *cavity2*, respectively; *HWP1* and *HWP2* are two half-wave plates; *DL* is time delay setup, for instance, fiber loops with the storage time T . At time $t = 0$, the working-state of switches $K1$ and $K2$ is transmitted and kept until time $t = T$; at time $t = T$, $K1$ and $K2$ are on reflected-state; $C1$ and $C2$ are two circulators.

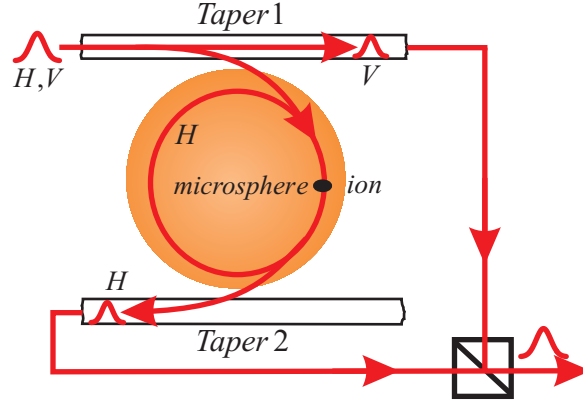


FIG. 2: Coupling between two fiber tapers and a microsphere, i.e. the realization of gate $U_{i,p}^{CPF}$. *Taper1* (*Taper2*) is input (output) coupler for H polarization component.

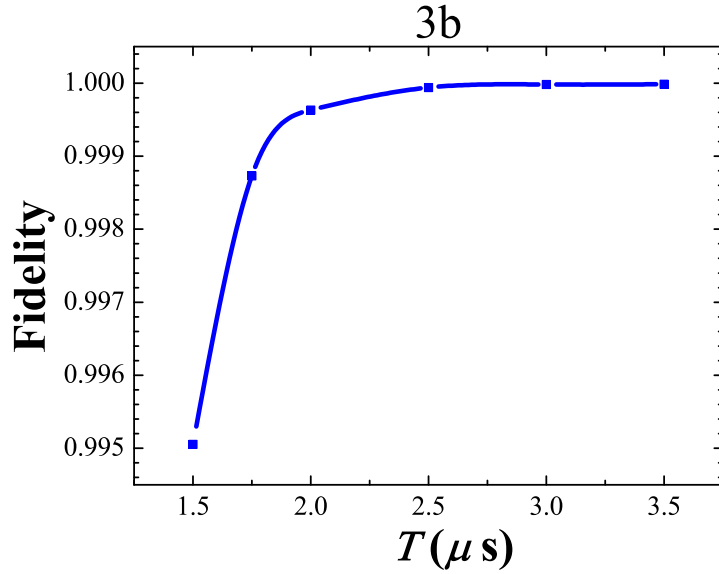
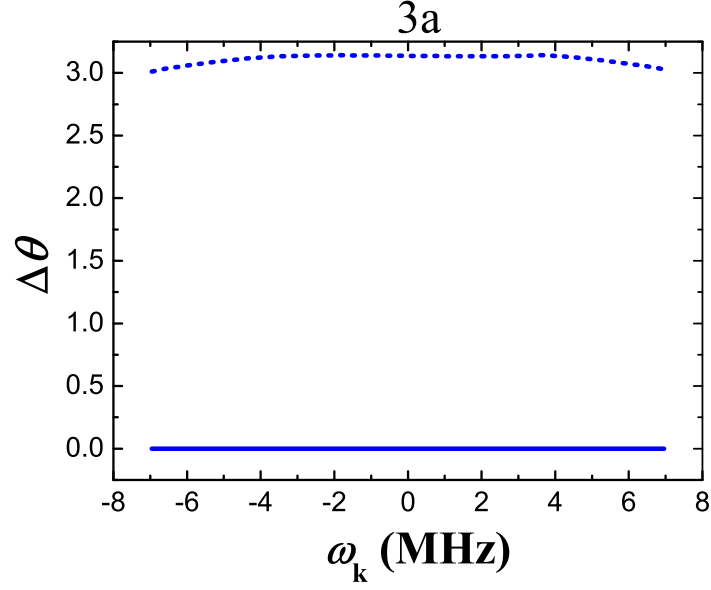


FIG. 3: (a) Phase variation after the single-photon pulse ($T = 3$) is reflected. Dashed (solid) curve depicts the phase change $\Delta\theta_{\omega_k}^{(0)}$ ($\Delta\theta_{\omega_k}^{(1)}$) when the ion is in $|0\rangle$ ($|1\rangle$). (b) Gate fidelity between a single ion and a single photon for different pulse duration T . Parameters for (a), (b), $g = 1.0$ GHz, $\kappa = 32$ MHz, $\gamma = 1$ kHz.